AJNR Am J Neuroradiol 22:670–676, April 2001

Variations of the Basal Vein: Identification Using Three-dimensional CT Angiography

Yasuhiro Suzuki, Hisato Ikeda, Motohiko Shimadu, Yoshiho Ikeda, and Kiyoshi Matsumoto

BACKGROUND AND PURPOSE: **The basal vein of Rosenthal (BVR) presents with many variations because of its origin in the secondary longitudinal anastomoses between embryonic veins. The variations were evaluated by 3D CT angiography imaging.**

METHODS: **Three-dimensional CT angiograms in the axial stereoscopic view and other directions constructed by the voxel transmission method and maximum intensity projection (MIP) images were obtained in 500 sides of 250 patients.**

RESULTS: **The BVR flowed into the great vein of Galen in 87.8%, but the anastomoses between the first and second segments were not confirmed in 36.9% of this type. The first segments with hypoplastic or aplastic anastomoses flowed into the cavernous sinus or the sphenoparietal sinus. Therefore, typical BVRs with these anastomoses accounted only for 55.4% of all sides. More than one fourth of the typical type also entered the anterior veins such as the cavernous sinus. Drainage was to the lateral mesencephalic vein in 5.6%, peduncular vein in 1.6%, and lateral or medial tentorial sinus in 5.0%.**

CONCLUSION: **Variations of the BVR can be classified on the basis of the five drainage pathways formed during the early embryonic stage. Three-dimensional CT angiography can show the stereoscopic anatomy and the main drainage routes, but not hypoplastic veins, which are only visible on MIP images.**

Information concerning the location and drainage pathway of the basal vein of Rosenthal (BVR) is important in the preoperative planning of skull base surgery. However, the BVR presents with many variations in course and drainage pathway (1–4), and such information is not easy to obtain by many of the current methods of investigation. This study investigated the variations of the BVR by using 3D CT angiography. We report on the utility of 3D CT angiography for the evaluation of this vein by using evaluation criteria based on its embryologic development.

Methods

Patients and Techniques

This study included 250 patients, 132 men and 118 women aged 28 to 85 years (mean age, 63.1 years), examined at our hospital between September 1996 and May 1999 for cerebrovascular disease, brain tumor, or abnormalities discovered during routine screening for cerebrovascular diseases and other intracranial diseases. No patient had CT signs of edema and midline shift or had undergone an operation.

Received June 13, 2000; accepted after revision September 28.

From the Department of Neurosurgery, Showa University, School of Medicine, 5-8 Hatanodai 1, Shinagawa-ku, Tokyo 142-8666, Japan.

Address reprint requests to Yasuhiro Suzuki, M.D.

Three-dimensional CT angiography was performed with a Hitachi W-2000 scanner (2 MHU-loaded, X-ray tube capacity) in helical mode. The X-ray tube's potential and current were 120 kV and 175 mA, respectively. The scanning parameters were a 2-mm slice thickness, a 1.3-mm/s table speed, and a 1-second scanning time. Nonionizing contrast material was injected intravenously at 3 mL/s for 33 seconds (100-mL total volume), and scanning was started 22 seconds after beginning the injection. Three-dimensional reconstruction used the voxel-transmission method with a threshold of 70–90 HU. The software provided with the CT scanner was used for 3D reconstruction without processing on a separate workstation. Axial stereoscopic images and oblique images in the bilateral anterior or posterior directions were reconstructed, as well as the anteroposterior and posteroanterior views in some cases. The stereoscopic view was composed of two images. There was a shift of approximately 15° in the horizontal direction between these two images. The axial images of the maximum intensity projection (MIP) method were also reconstructed.

The anatomy of the BVR was classified into three segments according to Huang and Wolf (3). The first segment extends from the union of the inferior striate vein, the anterior cerebral vein, and the deep middle cerebral vein to the anterior end of cerebral peduncle; the second segment extends to the union of the BVR and the lateral mesencephalic vein; and the third segment extends to the point draining into the great vein of Galen or the internal cerebral vein. According to this classification, the drainage pathways of each vein were evaluated.

Films rather than television monitor images were used for the evaluation so that all cases could be observed under the same conditions. The images were evaluated by the same neurosurgeon on two separate occasions. The observer had 17 years' experience as a neurosurgeon and has evaluated 3D CT angiograms since 1993. The veins could be distinguished from

TABLE 1: Summary of drainage pathways from the basal vein of Rosenthal (BVR)

Outflow Vessel	Second Segment	First Segment		Third Segment		Other Anastomosis		
						LMV	Ped	Tent
GVG	439	BVR	198		…	23	6	5
		CSs	133					
		BVR + CSs	71					
		Others	37					
LMV	28	BVR	15	GVG	19	…	0	1
		CSs	10	LMV	2			
		BVR + CSs	1	GVG + LMV	3			
		Others	2	Others	4			
Ped	8	BVR	6	GVG	0	0	…	0
		CSs	1	LMV	7			
		BVR + CSs	1	GVG + LMV	0			
		Others	0	Others	1			
Tent	25	BVR	10	GVG	10	0	0	…
		BVR + CSs	2	LMV	2			
		CSs	13	GVG + LMV	2			
		Others	0	Others	11			

Note.—First segment: the segment from the union of the deep middle cerebral vein, inferior striate vein, and other veins to the anterior tip of the cerebral peduncle. Second segment: the segment to the union between the BVR and lateral mesencephalic vein. Third segment: the segment to the union between the BVR and great vein of Galen.

LMV = lateral mesencephalic vein; Ped = peduncular vein; Tent = lateral or medial tentorial sinus; GVG = great vein of Galen; CSs = cavernous sinus, sphenoparietal sinus, or superficial middle cerebral vein.

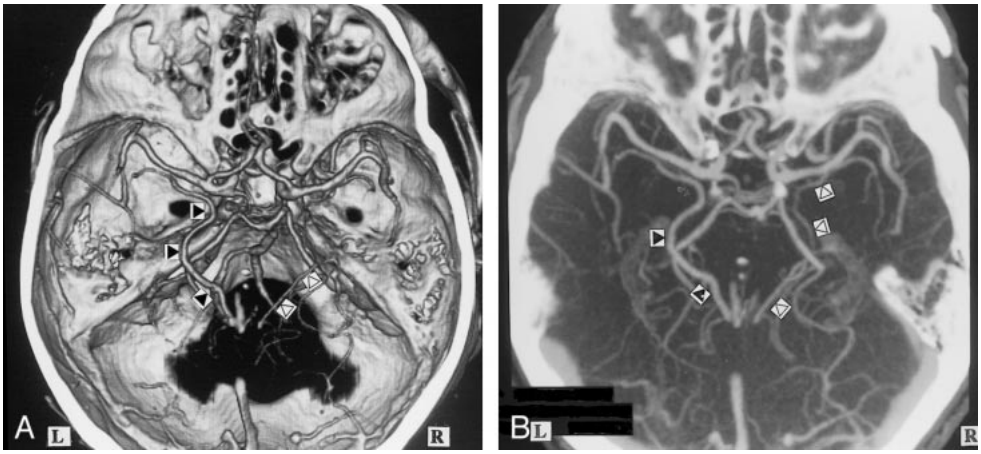

FIG 1. *A,* 3D CT angiogram (axial view) and *B,* MIP image. The left BVR (▲) typically courses posteriorly after receiving the deep middle cerebral vein. The anterior cerebral vein cannot be identified (*A*). The right BVR (△) is not depicted by 3D CT angiography (*A*), but is seen by MIP imaging (*B*).

the arteries by observing the stereoscopic view and the multiprojection view. If these two evaluations were not consistent, the result was regarded as obscure.

Results

The drainage routes of the second segment are shown in Table 1. The second segment was classified according to drainage directions into the great vein of Galen, the lateral mesencephalic vein, the pathway from the peduncular vein through the anterior pontomesencephalic vein to the superior petrosal sinus, and the pathway through the lateral or medial tentorial sinus to the transverse sinus or the straight sinus. The first segment was classified into flow in the anterior direction to the cavernous sinus, the sphenoparietal sinus, or the superficial middle cerebral vein; flow to the second segment; both of these routes; and obscure (Table 1). The third segment was classified as flow to the great vein of Galen, lateral mesencephalic vein, both of these routes, and others or obscure (Table 1).

The BVR flowed into the great vein of Galen in 87.8% (Fig 1) , but the anastomoses between the first segment and second segment were not confirmed in 36.9% of this type (Figs 2 and 3; Table 2). The first segments with such hypoplastic or aplastic anastomoses flowed into the cavernous sinus or sphenoparietal sinus. Therefore, typical BVRs with these anastomoses accounted for only 55.4% of all sides. More than one fourth of the

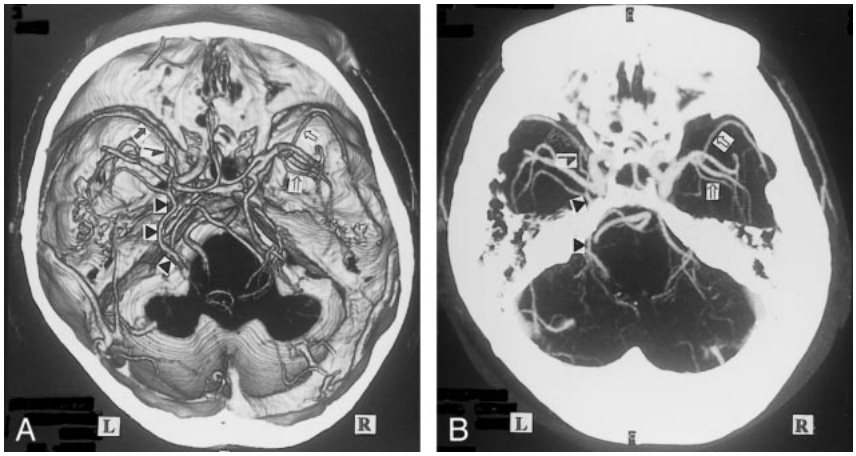

FIG 2. *A,* 3D CT angiogram (axial view) and *B,* MIP image. The left BVR (▲) enters the great vein of Galen, but communicates via the uncal vein (↱) with the superficial middle cerebral vein (⬆). The right deep middle cerebral vein (⇒) joins the superficial middle cerebral vein (⇧) and enters the cavernous sinus without forming the anastomosis between the first and second segment. This anastomosis is not visible on the MIP image.

FIG 3. *A,* 3D CT angiogram (axial view) and *B,* posteroanterior stereoscopic views. The right anterior cerebral vein (↑) and the deep middle cerebral vein (⇒) enter the sphenoparietal sinus via the uncal vein (↱) without forming the anastomosis between the first and second segment, and also communicate through the peduncular vein (≫) with the contralateral BVR and the anterior pontomesencephalic vein (>). The left BVR communicates via the uncal vein (↱) with the cavernous sinus, via the deep middle cerebral vein with the insular vein (⊥) and the superficial middle cerebral vein (⬆), via the peduncular vein (≫) with the anterior pontomesencephalic vein (>), and the great vein of Galen posteriorly.

TABLE 2: Summary of the basal vein of Rosenthal variations flowing into great vein of Galen

Anastomosis between First and Second Segment		Drainage Direction of First Segment		Other Anastomosis		
				LMV	Ped	Tent
Delineated	277	BVR	198	15	7	5
		BVR + CSs	73			
		Unknown	6			
Not delineated	162	CSs	135	8	1	1
		Others	3			
		Unknown	24			

Note.—LMV = lateral mesencephalic vein; Ped = peduncular vein; Tent = lateral or medial tentorial sinus; others = the draining vein or other drained veins could not be identified.

typical type also entered anterior sinuses or veins such as the cavernous sinus (Fig 2). Anastomoses between the first segment and the anterior vessels were found in 46.4% of all sides. The hypoplastic anastomosis was only depicted by the MIP image of many sides and appeared aplastic on the 3D CT angiograms (Fig 1). This disparity was also confirmed for the narrow parts of other segments and branches. Many BVRs that flowed into the great vein of Galen also anastomosed with the lateral

FIG 4. 3D CT angiogram (axial view). The right BVR flows through the lateral mesencephalic vein (⊥) to the superior petrosal sinus (SuPS) and enters the transverse sinus via the lateral or medial tentorial sinus (△). The left BVR enters the great vein of Galen (‡) and also flows into the lateral or medial tentorial sinus (▲).

mesencephalic vein, lateral or medial tentorial sinus, or peduncular vein (Figs 3–5). Other observed drainage patterns included the lateral mesencephalic vein in 5.6% (Fig 6), peduncular vein in 1.6% (Figs 3 and 7), and lateral or medial tentorial sinus in 5.0% (Fig 8). Anterior drainage routes such as the cavernous sinus persisted, not as the main route, but as supplements to the other routes. Many deep middle cerebral veins were identified on the 3D CT angiograms (Figs 3 and 7), but the anterior cerebral veins could not be seen even on the MIP images (Fig 1). The insular vein flowing through the deep middle cerebral vein into the BVR was delineated on many sides (Figs 2 and 3). Some BVRs of the lateral or medial tentorial sinus type coursed at the medial edge of tentorium and flowed into the straight sinus (Fig 8), and others flowed into the transverse sinus through the center or lateral side of the tentorium (Fig 4).

Discussion

The BVR presents with many variations because of its origin in the longitudinal anastomoses between veins in the early embryonic stages (1–4). Therefore, systematization of the variations tends to be hindered by this complex embryologic and ontogenic development. One institution is unlikely to examine enough cadavers to observe all of the many variations. Angiography cannot clearly delineate the venous phase or the 3D structure by limited-projection images. Three-dimensional CT angiography cannot reveal vessels of less than 1-mm diameter (5), but provides multidirectional stereoscopic images with specific vessel enhancement of the anatomic relationships with arteries and bone structure (6, 7). Consequently, 3D CT angiography seems to be the most suitable method for the inspection of venous variations (8, 9). The venous images of helical CT (otherwise called CT venography) (8, 10–12) generally provide superior venous delineation compared with MR venography (8, 9, 13–15). Multiplanar reconstruction (MPR) and MIP imaging are generally used rather than 3D imaging like the volume-rendering method. Three-dimensional CT angiography cannot delineate narrow vessels as well as MPR and MIP imaging can,

FIG 5. *A,* 3D CT angiogram (axial view) and *B,* posteroanterior stereoscopic views. The left BVR communicates with the great vein of Galen and lateral mesencephalic vein (⊥). The inferior ventricular veins (∀) originating from the choroid plexuses (†) are clearly seen bilaterally.

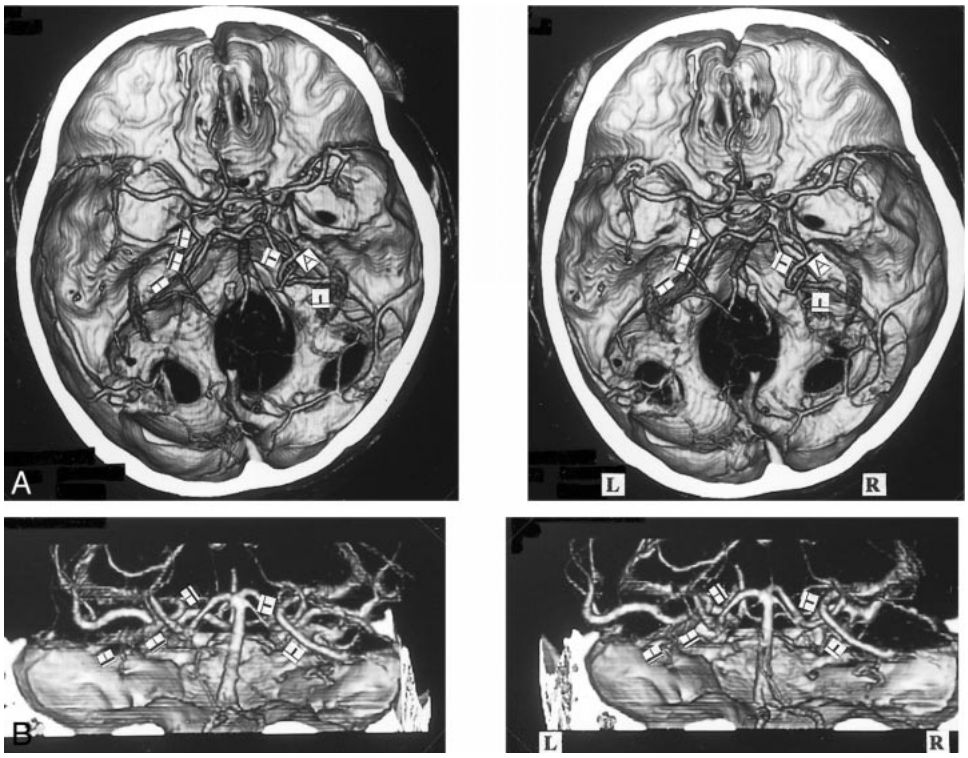

FIG 6. *A,* 3D CT angiogram (axial, stereoscopic views) and *B,* posteroanterior stereoscopic views. The bilateral BVRs drain via the lateral mesencephalic vein (⊥, ⊥) into the superior petrosal sinus. In the presence of a hypoplastic third segment of the BVR, the right inferior ventricular vein (∀) enters the lateral mesencephalic vein. The left third segment enters the great vein of Galen.

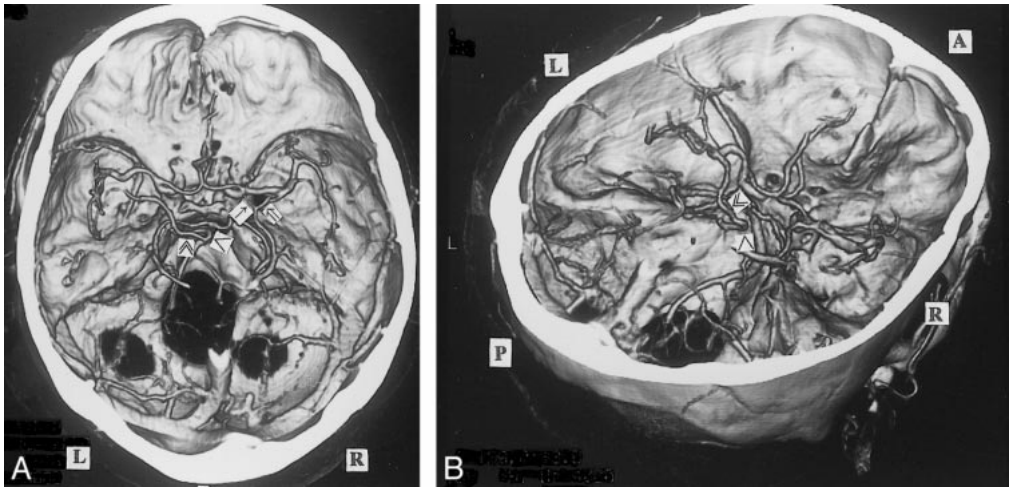

FIG 7. *A,* 3D CT angiogram (axial view) and *B,* right posterosuperior oblique view. The left BVR enters the superior petrosal sinus via the peduncular vein (≫) and anterior pontomesencephalic vein (>). The right first segment is formed from the union of the deep middle cerebral vein (⇒) and the anterior cerebral vein (↑).

but it is very useful for assessing the general anatomy of veins and their relationship with surrounding structures.

Padget's extraordinarily comprehensive and detailed investigation of the development of the cranial venous system showed that the BVR is a complex vessel formed secondarily as a longitudinal anastomotic channel that links up several veins of more primary embryologic significance (1). The components develop as the telencephalic vein, diencephalic vein, and mesencephalic vein in the 14- to 18-mm embryonic stage, and differentiate to the deep telencephalic vein, the ventral diencephalic vein, the dorsal diencephalic vein, and the mesencephalic vein (Fig 9). The BVR is formed by the anastomoses between these components in the 60- to 80-mm embryonic stage. Posterior drainage is formed by the connection between the dorsal diencephalic vein and the internal cerebral vein or the tributary of the great vein of Galen. The deep

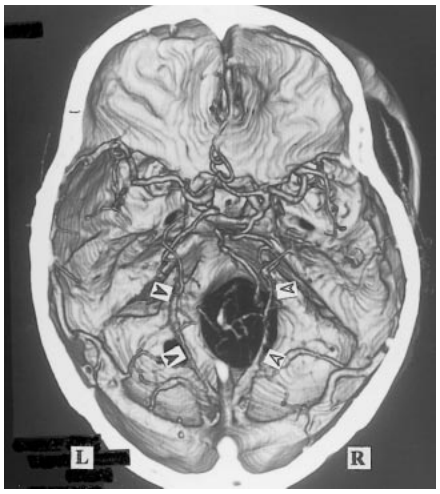

FIG 8. 3D CT angiogram (axial view). The bilateral BVRs course along the medial edge of the tentorium (▲, △) and enter the straight sinus. The first segment of the right BVR and the third segment of the left BVR cannot be confirmed.

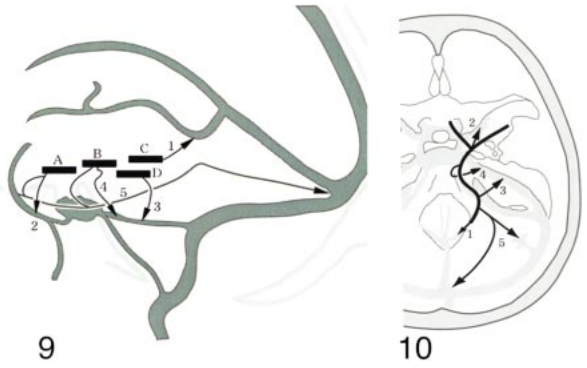

FIG 9. Four components constituting the BVR and the drainage pathways (1–5).

The components develop as the telencephalic vein, diencephalic vein, and mesencephalic vein in the 14- to 18-mm embryonic stage and differentiate to the deep telencephalic vein (*A*), the ventral diencephalic vein (*B*), and the dorsal diencephalic vein (*C*). The BVR is formed by the anastomoses between these components and the mesencephalic vein (*D*) during the 60- to 80- mm embryonic stage (Padget). Each primitive vein (four vessels) has one or more drainage pathways (five routes). The extent of the anastomoses and the drainage pathways result in a huge number of variations.

FIG 10. Longitudinal anastomoses of the primitive veins and the drainage routes of the BVR.

Five drainage pathways to be considered when the BVR is evaluated. 1: to great vein of Galen, 2: to cavernous sinus or sphenoparietal sinus, 3: to superior petrosal sinus via lateral mesencephalic vein, 4: to superior petrosal sinus via the peduncular vein, 5: to transverse sinus or straight sinus via the tentorium.

middle cerebral vein and the anterior cerebral vein develop from the deep telencephalic vein, and the ventral diencephalic vein begins to drain from the edge of the lesser sphenoid wing via the primitive tentorial sinus into the transverse sinus at approximately the 40-mm embryonic stage (1, 16). This primitive tentorial sinus drainage pathway remains for a while after birth, but as it dwindles, the drainage pathway of the superficial middle cerebral vein and deep middle cerebral vein proceeds to the route via the sphenoparietal sinus into the cavernous sinus. The ventral diencephalic vein forms the communication with the superior petrosal sinus via the peduncular vein and anterior pontomesencephalic vein in addition to the primitive tentorial sinus. The mesencephalic vein forms the lateral mesencephalic vein connecting with the ventral diencephalic vein on one side and the metencephalic vein (this vein finally develops to the superior petrosal sinus) on the other side (2, 3, 17). Although secondary embryonic anastomoses do not always form a single continuous vessel, these isolated primary vessels are present after birth and until the adult stage, so these developments result in many variations of the BVR (3, 4).

We compared the drainage routes or communications of the BVR identified from 3D CT angiograms with the drainage pathways of each primary vessel (Fig 10). As every observed side presented as one of the pathways or combinations, this embryologic classification enabled us to understand the systemic variations of the BVR very easily.

We propose that the potential variations of the BVR can be classified on the basis of these five drainage pathways, and the anastomoses between the primary primitive veins (deep telencephalic vein, ventral diencephalic vein, dorsal diencephalic vein, and mesencephalic vein). These combinations could potentially give rise to a myriad of variations. Consequently, this classification will facilitate the assessment of the systemic variations of the BVR, especially compared with attempts to describe copious, individual variations.

Discrimination of the BVR by MPR and MIP imaging has varied from 96% (8), 80% (18, 19), and 66% (10). We found that 3D CT angiography with MIP imaging could delineate the vein on all sides. Some BVR structures, which were not depicted by digital subtraction angiography, were unequivocally seen on CT scans (10). Flow and mixing phenomena of opacified and unopacified blood, and insufficient volume of contrast medium in the venous phase, may prevent identification of the vein by digital subtraction angiography. Many hypoplastic anastomoses between the first and second segments could not be recognized on 3D CT angiograms without the support of MIP images (Fig 1), and most branches flowing into the BVR, except for the inferior ventricular vein (Figs 6 and 9), could not be delineated consistently. These results indicate that even if the third segment is not identified or the flow to the great vein of Galen appears to be the only drainage pathway, we should consider the presence of narrow collateral vessels that are not detected by 3D CT angiography or MIP imaging. Therefore, the exact drainage pathways are difficult to classify, so we should recognize which of the five drainage routes is the main pathway. The presence of the BVR is best established by MIP imaging and the relationship with the surrounding structures by 3D CT angiography, which

provides more stereoscopic spatial venous information than angiography does. The BVR coursing laterally or medially and longitudinally is seen best on axial CT scans.

It is very important to identify the BVR variation present in each case. If the first segment enters the cavernous sinus via the uncal vein, the vein should be given special attention to avoid damage during the pterional approach. If the first segment enters the lateral mesencephalic vein or peduncular vein, the presence of a connecting vein between the middle and posterior cranial fossa should be considered in the subtemporal or lateral suboccipital approach. In the case of the lateral or medial tentorial sinus type, the information provided by the images is very useful for incision of the tentorium in the occipital transtentorial approach, and the images show the detailed drainage pattern and diameter of the third segment entering the great vein of Galen. Three-dimensional CT angiography is clearly useful for preoperative planning to identify the attention necessary for avoiding damage to the venous system.

Conclusion

The five drainage pathways formed during the early embryonic stage provide the basis for a simple classification of the many variations of the BVR. Three-dimensional CT angiography provides information on the systemic form and the main drainage pathway of the BVR despite problems with delineating hypoplastic anastomoses and narrow vessels. The BVR is best detected by MIP imaging and the relationship with the surrounding structures by stereoscopic 3D CT angiography, which provides more spatial venous information than angiography does.

References

1. Padget DH. **The cranial venous system in man in reference to development, adult configuration, and relation to the arteries.** *Am J Anat* 1956;98:307–355
2. Wolf BS, Huang YP, Newton CM. **The lateral anastomotic mesencephalic vein and other variants in drainage of the basal vein.** *AJR Am J Roentgenol* 1963;89:411–422
3. Huang YP, Wolf BS. **The basal cerebral vein and its tributaries.** In: Newton TH, Poos DG, eds. *Radiology of the Skull and Brain* (vol. 2, book 3). St. Louis, Mo: Mosby;1974:2111–2154
4. Ito J. **Supratentorial venous system.** In: Maki Y, Kuru H, eds. *Neuroradiology* I. Tokyo: Asakura Shoten;1986:443–484
5. Suzuki Y, Kawamata T, Matsumoto H, Matsumoto K. **[Detection of middle cerebral artery stenosis using 3D-CTA and MRA.]** *Jpn J Neurosurg* 1998;7:541–547 (Japanese, with English abstract)
6. Aoki S, Sasaki Y, Machida T, Ohkubo T, Minami M, Sasaki Y. **Cerebral aneurysms: Detection and delineation using 3-D-CT angiography.** *AJNR Am J Neuroradiol* 1992;13:1115–1120
7. Harbaugh RE, Schlusselberg DS, Jeffery R, Hayden S, Cromwell LD, Pluta D. **Three-dimensional computerized tomography angiography in the diagnosis of cerebrovascular disease.** *J Neurosurg* 1992;76:408–414
8. Casey SO, Alberico RA, Patel M, et al. **Cerebral CT venography.** *Radiology* 1996;198:163–170
9. Volg TJ, Bergman C, Villinger A, Einhaupl K, Lisser J, Felix R. **Dural sinus thrombosis: value of venous MR angiography for diagnosis and follow-up.** *AJR Am J Roentgenol* 1994;162:1191–1198
10. Wetzel SG, Kirsch E, Stock KW, Kolbe M, Kaim A, Raude EW. **Cerebral veins: Comparative study of CT venography with intraarterial digital subtraction angiography.** *AJNR Am J Neuroradiol* 1999;20:249–255
11. Kirchhof K, Jansen O, Sartor K. **CT-Angiographie der Hirnvenen.** *Rofo Fortschr Geb Rontgenstr Neuen Bildgeb Verfahr* 1996; 165:232–237
12. Hagen T, Bartylla K, Waziri A, Schmitz, Piepgras U. **Sterenwert der CT- Angiographe in der Diagnostik von zerebralen Sinus- und Venenthrombosen.** *Radiologe* 1996;36:859–866
13. Alberico R, Patel M, Casey S, Jacobs B, Maguire W, Decker R. **Evaluation of the circle of Willis with 3-D CT angiography in patients with suspected intracranial aneurysms.** *AJNR Am J Neuroradiol* 1995;16:1571–1578
14. Huston J III, Ehman JL. **Comparison of time-of-flight and phase-contrast MT neuroangiographic techniques.** *Radiographics* 1993;13:5–19
15. Mattle HP, Wentz KU, Edelman RR, et al. **Cerebral venography with MR.** *Radiology* 1991;178:453–458
16. Wolf BS, Huang YP, Newton CM. **The superficial sylvian venous drainage system.** *AJR Am J Roentgenol* 1963;89:398–410
17. Padget HD. **Development of cranial venous system in man, from view point of comparative anatomy.** *Contrib Embryol* 1957;36:79–140
18. Stein RL, Rosenbaum AE. **Deep supratentorial veins.** In: Newton TH, Potts DG, eds. *Radiology of the Skull and Brain, II: Angiography.* St. Louis, Mo: Mosby;1974:1903–1998
19. Huber P. ***Zerebrale Angiographe fur Klink und Praxis*** **(3rd ed).** Stuttgart: Thieme;1979:208–211